Producing and Exploiting Simultaneously the Forward and Backward Coupling in EBG-assisted Microstrip Coupled Lines

Jon Mikel Percaz, Magdalena Chudzik, Israel Arnedo, *Member, IEEE*, Ivan Arregui, *Member, IEEE*, Fernando Teberio, Miguel A. G. Laso, *Senior Member, IEEE*, and Txema Lopetegi, *Member, IEEE*

***Abstract*— In this paper, a methodology is proposed for the design of EBG-assisted coupled line structures in microstrip technology, controlling independently the forward and backward coupling. It is based on the use of a single-frequency-tuned electromagnetic bandgap (EBG) structure to produce a single backward-coupled frequency band, in combination with the forward-coupled frequency bands produced by the difference between the even and odd mode propagation constants present in microstrip technology. Thus, the central frequency of the backward-coupled band is controlled by the period of the EBG structure, while the frequencies of the forward-coupled bands are fixed by the length of the device. The rest of the frequencies go to the direct port giving rise to a device with the input port matched at all the frequencies and where the coupled bands are easily controllable by adjusting the corresponding design parameter. The novel methodology proposed has been successfully demonstrated by designing a triplexer intended for the GSM (900 MHz) and WLAN (2.4 GHz and 5.5 GHz) telecommunication bands.**

***Index Terms*—Coupled lines, electromagnetic bandgap (EBG), coupled mode theory, microstrip circuits, triplexer.**

I. Introduction

Coupled lines have been widely used at microwave and millimeter wave frequencies for a long time, with very important applications like the implementation of directional couplers, filters, and transformers [1], [2]. Two different coupling mechanisms have been identified for the coupled line structures: the backward coupling and the forward coupling. Depending on the coupling mechanism employed the structures are classified into two different groups [1-3]. The first group comprises the coupled line structures that couple the energy to the port adjacent to the input port (through a wave propagating in the backward direction) and are based on the use of different even and odd characteristic impedances. The second group includes the structures that couple the energy to the port adjacent to the direct port (through a wave propagating in the forward direction) and are based on the use of different even and odd propagation constants [4]. In both groups the length of the structure controls the central frequency of the coupled band and only the corresponding mechanism (backward or forward coupling) is exploited [2].

This work was supported by MINECO (Spain) under projects TEC2011-28664-C02-01 and TEC2014-51902-C2-2-R.
J. M. Percaz, M. Chudzik, I. Arnedo, I. Arregui, F. Teberio, M. A. G. Laso, and T. Lopetegi are with the Electrical and Electronic Engineering Department, Public University of Navarre, 31006 Pamplona, Navarre, Spain (e-mail: txema.lopetegi@unavarra.es).

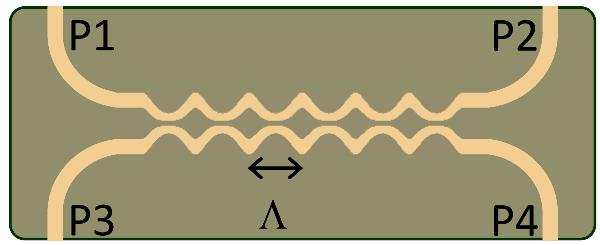

Fig. 1. Schematic of the EBG-assisted coupled line structure with EBG period Λ. The ground plane is kept unaltered.

In this paper a methodology is proposed to produce and exploit simultaneously the forward and backward coupling in coupled line structures. In contrast with the classical designs, the backward coupling will be achieved by introducing an EBG structure, allowing us to obtain strong coupling and a single backward-coupled band whose central frequency is independent of the length of the structure [5], [6]. A technology with distinct even and odd propagation constants will be used to obtain the forward-coupled bands. Recently, a related EBG structure has been also successfully demonstrated but for differential microstrip lines, with the very different application of common-mode suppression, and consequently with very different design methodology and operation [7].

The operation principle of the EBG-assisted coupled line structure proposed here, with independent control of the couplings, rests on the fact that the signal introduced in the input port (P1) is backward-coupled to P3 by the EBG structure, and forward-coupled to P4 by the difference between the even and odd propagation constants, see Fig. 1. The central frequency of the single backward-coupled band obtained in P3 depends on the period of the EBG structure, Λ, while the central frequencies of the forward-coupled bands obtained in P4 are determined by the total length of the device. The rest of the frequencies go to the direct port (P2), ensuring good matching at the input port (P1) for all the frequencies.

The microstrip technology has been selected for the implementation of the device since it fulfills the condition of distinct even and odd propagation constants required, and it ensures low cost, direct integration, and easy fabrication using printed circuit technology.

II. Design of EBG-assisted Coupled Line Structures

An EBG structure is implemented in coupled line technology by introducing an adequate periodic variation of the coupled strips width and separation. The resulting four-port side-by-side symmetrical device (see Fig. 1) can be studied employing the even and odd modes of the coupled line structure. Taking advantage of this mode decomposition, the frequency dependent *S*-parameters of the four-port device can be calculated as [2]:

$$S_{11}(f)=\frac{\Gamma_e(f)+\Gamma_o(f)}{2};\quad S_{31}(f)=\frac{\Gamma_e(f)-\Gamma_o(f)}{2} \tag{1}$$

$$S_{21}(f)=\frac{\mathrm{T}_e(f)+\mathrm{T}_o(f)}{2};\quad S_{41}(f)=\frac{\mathrm{T}_e(f)-\mathrm{T}_o(f)}{2} \tag{2}$$

where $\Gamma_e(f)$ and $\Gamma_o(f)$ are the reflection coefficients of the even and odd modes, respectively, $\mathrm{T}_e(f)$ and $\mathrm{T}_o(f)$ are the transmission coefficients of the even and odd modes, and the port numbers follow the convention shown in Fig. 1.

As it can be seen in (1), if the design condition

$$\Gamma_e(f)=-\Gamma_o(f) \tag{3}$$

is satisfied, then $S_{11}(f) = 0$ and $S_{31}(f) = \Gamma_e(f)$, producing a device with the input port P1 matched at all the frequencies and where the EBG stopband is backward-coupled to P3. Using the coupled mode theory [8], [9], the electromagnetic behavior of the EBG-assisted coupled line structure can be characterized through the even and odd coupling coefficients, $K_e(z)$ and $K_o(z)$. As it is explained in [10], if a sinusoidal function for $K_e(z)$ is employed:

$$K_e(z)=A\cdot\sin\left(\frac{2\cdot\pi}{\Lambda}\cdot z\right) \tag{4}$$

then a spurious-free EBG structure that features only the fundamental backward-coupled band is obtained. Thus, a simple design formula to calculate the EBG period, Λ (see Fig. 1), from the central frequency f_{31} of the single backward-coupled band can be obtained [10], [5]:

$$\Lambda=\frac{c}{2\cdot f_{31}\cdot\sqrt{\varepsilon_{eff}}} \tag{5}$$

as well as expressions for the coupling level, $|S_{31}(f_{31})|$, and bandwidth between zeros, BW_{31}, of the coupled band:

$$|S_{31}(f_{31})|=\tanh(A\cdot L/2) \tag{6}$$

$$BW_{31}=\frac{c}{\pi\cdot\sqrt{\varepsilon_{eff}}}\cdot\sqrt{\left(\frac{A}{2}\right)^2+\left(\frac{\pi}{L}\right)^2} \tag{7}$$

where c is the speed of light in vacuum, L is the device length and ε_{eff} is the mean value of the effective dielectric constant along the device. It is important to highlight that by using the EBG structure the central frequency of the backward-coupled band, f_{31}, is fully independent of L.

Considering now the transmission coefficients $\mathrm{T}_e(f)$ and $\mathrm{T}_o(f)$ used in (2), it is important to notice that out of the single backward-coupled band, the reflection coefficients $\Gamma_e(f)$ and $\Gamma_o(f)$ will be negligible since the reflection is governed by the spurious-free EBG structure carefully designed to forbid propagation only around f_{31}. Therefore, out of the single backward-coupled band, the magnitudes of $\mathrm{T}_e(f)$ and $\mathrm{T}_o(f)$ will be approximately equal to 1, while their phases will be a product, with minus sign, of the propagation constant of the even or odd mode, β_e or β_o, respectively, and the length of the device, L. Inspecting (2), it can be seen that if $\mathrm{T}_e(f_{41}) = -\mathrm{T}_o(f_{41})$, with magnitudes equal to 1, then $|S_{41}(f_{41})| = 1$ and the signal with frequency f_{41} will be forward-coupled to P4. This condition will be satisfied when:

$$\beta_e\cdot L-\beta_o\cdot L=m\cdot\pi \tag{8}$$

where m = 1, 3, 5,…, and will give rise to a full coupling of the energy to P4 at the corresponding frequencies.

The length necessary for the EBG-assisted coupled line structure to get the first forward-coupled band to P4 at the frequency f_{41} is obtained from (8) when m = 1, as [2]:

$$L=\frac{c}{2\cdot f_{41}\cdot(\sqrt{\varepsilon_{eff,e}}-\sqrt{\varepsilon_{eff,o}})} \tag{9}$$

where $\varepsilon_{eff,e}$ and $\varepsilon_{eff,o}$ are the mean even and odd effective dielectric constants along the device (directly associated to β through the expression $\beta=2\pi f/c\cdot\sqrt{\varepsilon_{eff}}$). For higher values of m = 3, 5, 7,…, additional forward-coupled bands will be obtained at the frequencies $m\cdot f_{41}$, see (8). Moreover, when m = 0, 2, 4,…, then $\mathrm{T}_e(f)$ and $\mathrm{T}_o(f)$ will be in phase, see (8), and if their magnitudes are equal to 1 then $\mathrm{T}_e(f_{21}) = \mathrm{T}_o(f_{21})$ and $|S_{21}(f_{21})| = 1$, see (2). As a result, the signal with frequency f_{21} will be fully routed to the direct port (P2), where f_{21} can take the values $m\cdot f_{41}$ with m = 0, 2, 4,… It should be noted that in order to avoid the need of an excessive length for the device, a significant difference between $\varepsilon_{eff,e}$ and $\varepsilon_{eff,o}$ is necessary in the implementation technology.

In general, for the frequencies out of the single backward-coupled band produced by the EBG structure (where the magnitudes of $\mathrm{T}_e(f)$ and $\mathrm{T}_o(f)$ are approximately equal to 1), the frequency behavior of the forward-coupled bands, $|S_{41}(f)|$, and of the direct bands, $|S_{21}(f)|$, is given by [2]:

$$|S_{41}(f)|=\sin\left[\frac{\pi\cdot L\cdot f\cdot\left(\sqrt{\varepsilon_{eff,e}}-\sqrt{\varepsilon_{eff,o}}\right)}{c}\right] \tag{10}$$

$$|S_{21}(f)|=\cos\left[\frac{\pi\cdot L\cdot f\cdot\left(\sqrt{\varepsilon_{eff,e}}-\sqrt{\varepsilon_{eff,o}}\right)}{c}\right] \tag{11}$$

The expression that relates the physical dimensions of the device and its coupling coefficient can be given (for our case of TEM or quasi-TEM modes) as a function of the characteristic impedance [8], [9]:

$$K(z) = -\frac{1}{2}\cdot\frac{1}{Z_0}\cdot\frac{dZ_0}{dz} \tag{12}$$

By solving analytically the equation, the even characteristic impedance profile, $Z_{0e}(z)$, necessary to implement the designed EBG-assisted coupled line structure with sinusoidal even coupling coefficient, see (4), can be obtained:

$$Z_{0e}(z) = Z_{0e}(0)\cdot e^{-\frac{A\cdot\Lambda}{\pi}\cdot\left[\cos\left(\frac{2\cdot\pi}{\Lambda}\cdot z\right)-1\right]}, \quad z\in[0,L] \tag{13}$$

where $Z_{0e}(0)$ is the $Z_{0e}(z)$ value at the beginning of the device, and Λ and L are calculated using (5) and (9), respectively, to obtain the backward- and forward-coupled bands around the frequencies f_{31} and f_{41}, respectively. The amplitude parameter, A, controls the coupling level, $|S_{31}(f_{31})|$, and bandwidth between zeros, BW_{31}, of the backward-coupled band through (6) and (7), as explained above, and fixes the maximum value for $Z_{0e}(z)$:

$$Z_{0e\max} = Z_{0e}(0)\cdot e^{2\cdot\frac{A\cdot\Lambda}{\pi}} \tag{14}$$

Regarding the odd mode, by applying the design condition (3) imposed at the beginning of this section, and the sign inversion property reported in [8], the following equality is obtained:

$$K_e(z) = -K_o(z) \tag{15}$$

Thus, the odd characteristic impedance, $Z_{0o}(z)$, must follow the profile in (13), but with the opposite sign in the exponent [10], [5].

Finally, a tapering function, $T(z)$, is applied to the $Z_{0e}(z)$ and $Z_{0o}(z)$ profiles in order to smoothly adjust the values of the characteristic impedances at the ports P2 and P4, when a non-integer number of periods is necessary to complete the calculated device length, L. Additionally, the tapering function minimizes the ripple (side-lobe level) produced in frequency by the EBG structure, but it also reduces the level of energy coupled throughout the EBG and, consequently, the length L employed in (6) and (7) needs to be replaced by the effective length of the tapered EBG structure that can be calculated as [11]:

$$L_{eff} = L\cdot A_{eff} = L\cdot\int_{-0.5}^{0.5} T(z)\cdot dz \tag{16}$$

where $T(z)$ is the normalized tapering function with amplitude and lengths equal to 1, and A_{eff} the area below it. Moreover, due to the fact that the even and odd modes propagate at different speeds, the Z_{0e} and Z_{0o} profiles are redistributed along the propagation direction using the $\varepsilon_{eff,e}$ and $\varepsilon_{eff,o}$ values in such a way that both modes are affected at each time instant by the same pair of impedances as in the case of equal speed propagation. The details about the algorithm employed are given in [12]. In this way, the design condition (3) is still satisfied in our device, although the even and odd modes feature different propagation constants.

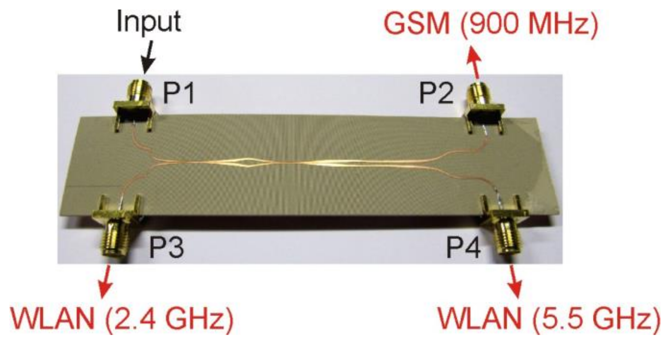

Fig. 2. Photograph of the microstrip triplexer, with labeled ports, implemented using an EBG-assisted coupled line structure.

The physical parameters of the EBG-assisted microstrip coupled-line structure (strip width and separation) are finally calculated from the obtained $Z_{0e}(z)$ and $Z_{0o}(z)$ profiles using the expressions available in [2] and *Agilent ADS LineCalc* tool, where even the thickness of the metallic strips is taken into account.

III. Example of Application: GSM and WLAN Triplexer

As an example of application, a microstrip triplexer working at GSM900 (f_{21} = 900 MHz) and both WLAN bands (f_{31} = 2.4 GHz and f_{41} = 5.5 GHz) has been designed using an EBG-assisted coupled line structure, see Fig. 2. The substrate employed is Rogers RO3010 (ε_r = 10.2, h = 0.635 mm) with 50 Ω input and output ports. The minimum separation between the metallic strips is fixed to 25 µm, which results in a maximum $Z_{0e}(z)$ value of Z_{0emax}=109.7 Ω (calculated using *Agilent ADS LineCalc*), guaranteeing a large value for the A parameter (see (14)) and consequently a high backward-coupling level, see (6). Again, using *Agilent ADS LineCalc*, the effective permittivities $\varepsilon_{eff,e}$ = 7.1 and $\varepsilon_{eff,o}$ = 5.7 are obtained for f_{31} = 2.4 GHz, resulting in a mean value of ε_{eff} = 6.4. Taking $Z_{0e}(0)$ = 50.5 Ω and $Z_{0o}(0)$ = 49.5 Ω for convenience, and using (5) and (14), the parameters to fix the $Z_{0e}(z)$ and $Z_{0o}(z)$ profiles (13) to get the backward-coupled band at f_{31}= 2.4 GHz are obtained: Λ = 24.8 mm, A = 49.2 m^{-1}. The device length is calculated using (9) to get a forward-coupled band at f_{41} = 5.5 GHz, with $\varepsilon_{eff,e}$ = 7.3 and $\varepsilon_{eff,o}$ = 5.6. The result obtained is L = 81.3 mm, which gives a number of periods of 3.3. The direct band will be placed around 0 GHz ($m\cdot f_{41}$, with m = 0), encompassing the intended value of f_{21} = 900 MHz. Due to the non-integer number of periods, and to minimize the ripple introduced in frequency by the EBG structure, an asymmetrical Bohman window [13] is applied over the $Z_{0e}(z)$ and $Z_{0o}(z)$ profiles. Finally, the spatial redistribution process is applied to $Z_{0e}(z)$ and $Z_{0o}(z)$ as explained in Section II, see Fig. 3. The designed device has been simulated using *CST Microwave Studio*, fabricated with a *LPKF ProtoLaser 200* laser PCB milling machine (see Fig. 2), and measured by means of an *Agilent™ 8722 VNA*. The results are shown in Fig. 4 and Fig 5.

This is the author's version of an article that has been published in this journal. Changes were made to this version by the publisher prior to publication.
The final version of record is available at http://dx.doi.org/10.1109/LAWP.2015.2478595

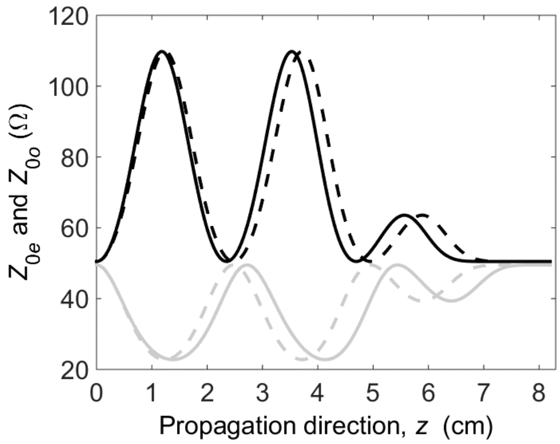

Fig. 3. Even (black line) and odd (grey line) characteristic impedances before (dashed line) and after (solid line) the spatial redistribution process.

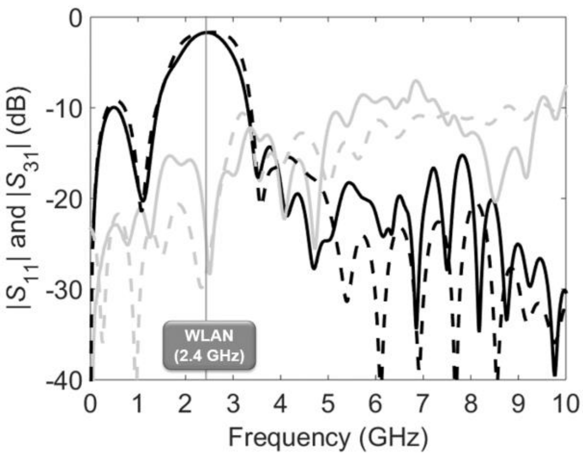

Fig. 4. Simulated (dashed line) and measured (solid line) $|S_{11}|$ (grey line) and $|S_{31}|$ (black line) parameters for the triplexer. The WLAN band operating at 2.4-2.45 GHz (IEEE 802.11b/g) backward-coupled to P3 is shaded in grey.

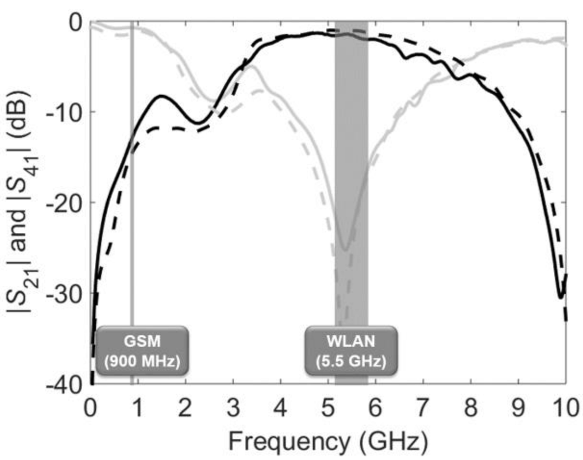

Fig. 5. Simulated (dashed line) and measured (solid line) $|S_{21}|$ (grey line) and $|S_{41}|$ (black line) parameters for the triplexer. The GSM band operating at 890-960 MHz (GSM900) directed to P2 and the WLAN band operating at 5.15-5.85 GHz (IEEE 802.11a) forward-coupled to P4 are shaded in grey.

A very good agreement is achieved between the simulated and measured results. As it can be seen, the input port (P1) is matched at all the frequencies, while the bands around f_{21} = 900 MHz, f_{31} = 2.4 GHz, and f_{41} = 5.5 GHz, are routed to the ports P2, P3, and P4, respectively, as intended, with measured coupling levels of $|S_{21}(f_{21})|$ = -0.7 dB, $|S_{31}(f_{31})|$ = -1.7 dB, and $|S_{41}(f_{41})|$ = -1.5 dB. The differences with the theoretical coupling levels (-0.2 dB, -0.8 dB, and 0 dB), calculated using (11), (6), and (10), respectively, can be attributed to the conductor and dielectric losses.

IV. Conclusion

A methodology for the design of EBG-assisted coupled line structures, that allows us to control and exploit simultaneously the forward and backward coupling, has been proposed. The structure obtained has its input port matched for all the frequencies. Several analytical expressions are given to calculate the design parameters, making the design procedure simple and straightforward. The novel technique has been validated with the design of a triplexer for the GSM and WLAN telecommunication bands, demonstrating good performance. Different coupling levels and bandwidths could be also achieved by employing the expressions obtained throughout the paper (6), (7), (10), (11).

References

[1] B. M. Oliver, "Directional Electromagnetic Couplers," *Proceedings of the I.R.E.*, vol. 42, pp. 1686-1692, Nov. 1954.
[2] R. Mongia, I. Bahl, P. Bhartia, and J. Hong, *RF and Microwave Coupled-Line Circuits. Boston*. Norwood, MA: Artech House, 2007.
[3] H. Mextorf, R. Knochel, "The intrinsic impedance and its application to backward and forward coupled-line couplers," *IEEE Trans. Microw. Theory Tech.*, vol. 62, no. 2, pp. 224-233, Feb. 2014.
[4] P. K. Ikalainen, G. L. Matthaei, "Wide-band, forward-coupling microstrip hybrids with high directivity," *IEEE Trans. Microw. Theory Tech.*, vol. 35, no. 8, pp. 719-725, Aug. 1987.
[5] M. Chudzik, I. Arnedo, A. Lujambio, I. Arregui, F. Teberio, M. A. G. Laso, and T. Lopetegi, "Microstrip coupled-line directional coupler with enhanced coupling based on EBG concept," *Electronics Letters*, vol. 47, no. 23, pp. 1284-1286, Nov. 2011.
[6] M. Chudzik, I. Arnedo, A. Lujambio, I. Arregui, F. Teberio, D. Benito, T. Lopetegi, M. A. G. Laso, "Design of EBG microstrip directional coupler with high directivity and coupling," *Proc. 42nd European Microwave Conference*, pp. 483-486, Oct.-Nov. 2012.
[7] P. Velez, J. Bonache, F. Martin, "Differential Microstrip Lines with Common-Mode Suppression Based on Electromagnetic Band-Gaps (EBGs)," *IEEE Antennas Wireless Propagation Letters*, vol. 14, pp. 40-43, 2015.
[8] I. Arnedo, M. A. G. Laso, F. Falcone, D. Benito and T. Lopetegi, "A series solution for the single mode synthesis problem based on the coupled mode theory," *IEEE Transactions on Microwave Theory and Techniques*, vol. 56, no. 2, pp. 457-466, Feb. 2008.
[9] T. Lopetegi, M. A. G. Laso, M. J. Erro, M. Sorolla, and M. Thumm, "Analysis and design of periodic structures for microstrip lines by using the coupled mode theory," *IEEE Microwave and Wireless Components Letters*, vol. 12, no. 11, pp. 441-443, Nov. 2002.
[10] I. Arnedo, M. Chudzik, J. D. Schwartz, I. Arregui, A. Lujambio, F. Teberio, D. Benito, M. A. G. Laso, D. V. Plant, J. Azaña, and T. Lopetegi, "Analytical solution for the design of planar EBG structures with spurious-free frequency response," *Microw. Opt. Technol. Lett.*, vol. 54, no. 4, pp. 956–960, Apr. 2012.
[11] M. A. G. Laso, M. J. Erro, T. Lopetegi, D. Benito, M. J. Garde, and M. Sorolla, "Optimization of Tapered Bragg Reflectors in Microstrip Technology," *International Journal of Infrared and Millimeter Waves*, vol. 21, no. 2, pp. 231-245, Feb. 2000.
[12] M. Chudzik, I. Arnedo, A. Lujambio, I. Arregui, I. Gardeta, F. Teberio, J. Azana, D. Benito, M. A .G. Laso, and T. Lopetegi, "Design of Transmission-Type Nth-Order Differentiators in Planar Microwave Technology," *IEEE Transactions on Microwave Theory and Techniques*, vol. 60, no. 11, pp. 3384-3394, Nov. 2012.
[13] H. Bohman, "Approximate Fourier analysis of distribution functions," *Arkiv för Matematik*, vol. 4, no. 2-3, pp. 99-157, 1960.